

# PATTERN SPEEDS OF SPIRAL GALAXIES USING THE TREMAINE-WEINBERG METHOD

S. E. Meidt<sup>1</sup> and R. J. Rand<sup>1</sup>

<sup>1</sup>*University of New Mexico*

## Introduction

Long-lasting spiral structure in galaxies is established when density waves form a pattern that rotates at a constant angular frequency  $\Omega_p$ , the pattern speed. This quantity, critical to understanding spiral structure, galaxy evolution, and the connection, if any, between bars and spirals in galaxies, is not directly measurable. Most determinations of pattern speeds have relied on identifying morphological features at certain radii as resonances, but this depends significantly on knowledge of the behavior of stars and gas at these resonances. The Tremaine-Weinberg (TW) method allows for the determination of pattern speeds based on kinematic observations in a way completely independent of resonance identification, or theories of spiral structure, relying on the identification of a tracer that obeys the continuity equation as it orbits through the pattern.

This work expands on previous studies of the TW method applied to galaxies with molecular- or HI-dominated ISMs. In galaxies where the ISM is found to be dominated by one phase, it is assumed that this component satisfies the continuity requirement; for galaxies with H<sub>2</sub> dominated ISMs, for instance, the TW method has successfully been applied using <sup>12</sup>CO(1-0) emission as a tracer for the molecular gas surface density (Rand & Wallin 2004).

## 1. The Tremaine-Weinberg Method

If the component obeys continuity as it orbits in the spiral/bar potential, Tremaine & Weinberg (1984) show that

$$\Omega_p \sin i = \frac{\int_{-\infty}^{\infty} \Sigma(X, Y) V_{\parallel} dX}{\int_{-\infty}^{\infty} \Sigma(X, Y) X dX}, \quad (1)$$

where  $(X, Y)$  are the sky coordinates  $\parallel$  and  $\perp$  to the major axis;  $\Sigma(X, Y)$  is the surface density of the component;  $V_{\parallel}$  is the line-of-sight velocity; and  $i$  is the inclination angle of the galaxy.

If the intensity of the component's emission traces the surface density, then, at a given  $Y$  (cf. Merrifield & Kuijken 1995),

$$\Omega_p = \frac{1}{\sin i} \frac{\int_{-\infty}^{\infty} I(X) V_{\parallel} dX}{\int_{-\infty}^{\infty} I(X) X dX} \frac{\int_{-\infty}^{\infty} I(X) dX}{\int_{-\infty}^{\infty} I(X) dX}, \quad (2)$$

and  $\Omega_p$ , modulo  $\sin i$ , can be determined from total intensity and velocity field maps by measuring intensity-weighted averages of observed position  $\langle x \rangle$  and velocity  $\langle v \rangle$  along lines of constant  $Y$  (parallel to the major axis). The slope in a plot of  $\langle v \rangle$  vs.  $\langle x \rangle$  for such "apertures" is the pattern speed.

## 2. Data and Analysis

Presently, to determine the spiral density wave pattern speed, we use high-resolution CO data cubes from the BIMA Survey of Nearby Galaxies (SONG). The BIMA SONG observations include single-dish data, thereby sampling all spatial frequencies to support the continuity requirement. Pattern speed determinations for three of the galaxies in this work are presented based on CO emission data cubes alone; we cite the results of Wong & Blitz (2002) wherein radial profiles of NGC 5055, 5033, and 5457 (M101) indicate that these galaxies are molecule-dominated within the region of CO detection.

In this work, a constant conversion factor  $X=2 \times 10^{20} \text{ mol cm}^{-2} (\text{K km s}^{-1})^{-1}$  between CO intensity and  $\text{H}_2$  column density is assumed. As demonstrated in Zimmer, Rand & McGraw (2004), the choice of conversion factor has little effect on the TW calculation. The choice, however, clearly influences assertions of molecular dominance, particularly with regard to an important suspected variation of  $X$  with metallicity, which is supported by empirical evidence for an inverse correlation (e.g. Boselli, Lequeux, & Gavazzi 2003). For the galaxies studied here, NGC 5457, 5055 and 5033, metallicity estimates are subsolar (as compiled by Pilyugin, et al. 2004), indicating that, if anything, the conversion factor underestimates the amount of  $\text{H}_2$  present.

Inclination and position angles (PA's) used in the TW calculation are determined by fitting tilted rings to the velocity field as performed by the GIPSY task ROTCUR. As found in Debattista (2003) and Rand & Wallin (2004), the scatter in the slope of the  $\langle v \rangle$  vs.  $\langle x \rangle$  plot worsens for PA's further from the nominal value. Error bars reported for the pattern speed of each galaxy account for PA uncertainty and the scatter in the  $\langle v \rangle$  vs.  $\langle x \rangle$  plot for nominal PA.

	Morphological Type	D (Mpc)	i (°)	PA (°)	$V_{sys}$ (km/s)	$\Omega_p$ (km/s/kpc)
NGC 5457	SAB(rs)cd	7.4	21	42 +4/-2	257	48 +7/-6
NGC 5055	SA(rs)bc	7.2	57	99 ±1	506	67 ±6
NGC 5033	SA(s)c	11.8	68	352 ±2	880	93 +18/-39

Table 1. Properties of sample galaxies.

### 3. Results

Given that NGC 5457, 5055 and 5033 appear to be dominated by molecular gas in their inner disks, we can be reasonably confident that the continuity requirement of the TW method is satisfied. Table 1 lists the properties and results of the TW calculation for each of the galaxies in our sample. Figures 1a and b display an example of the line-of-sight apertures used in the TW calculation for NGC 5457 and the corresponding  $\langle v \rangle$  vs.  $\langle x \rangle$  plot, respectively.

### 4. Conclusions and Future Work

The Tremaine-Weinberg method has long been applied with much success to bars in galaxies. The relatively recent applications of the method to spiral patterns, too, are compelling: pattern speeds for M51 and M83, for example (Rand & Wallin 2004), were found to be in good agreement with those determined from resonances. Generally, however, it is unclear how reliable spi-

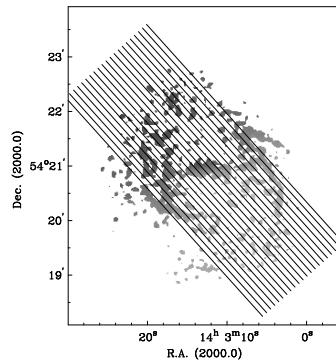


Figure 1a. First moment map of the BIMA CO data for NGC 5457 with apertures used in the TW calculation spaced at the resolution of the map shown overlaid as solid lines, with the westernmost being aperture 1.

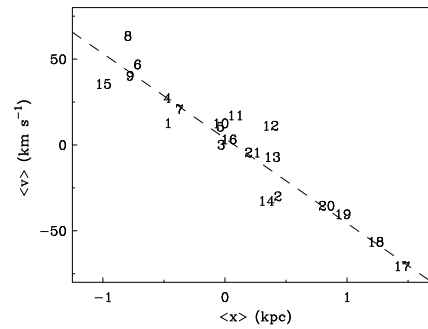
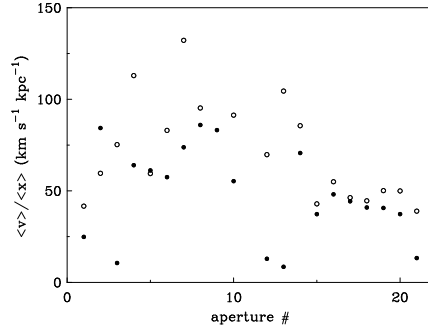


Figure 1b. Plot of  $\langle v \rangle$  vs.  $\langle x \rangle$  for the 21 apertures shown in fig. 1a. The dashed line is the best-fit straight line to all apertures. The corresponding value of  $\Omega_p$  is 48 +7/-6 km s<sup>-1</sup> kpc<sup>-1</sup>.



*Figure 2* Plot of  $\langle v \rangle / \langle x \rangle$  vs. aperture number for NGC 5457 with filled and open circles representing values from the TW calculation using the original and axisymmetric velocity fields, respectively.

ral pattern speed determinations with the TW method are, considering that the converging and diverging flows responsible for the pattern are typically weaker in a spiral (e.g. Roberts & Stewart 1987) than in a bar; the method, based on the continuity equation, relies on the detection of such non-axisymmetric, or "streaming", motions that trace spiral arm surface density enhancements in order to calculate a pattern speed. It is easy to show, in the case of purely axisymmetric azimuthal motion, that the method returns a weighted average of the angular rotation frequency. This makes sense: in such a case, only a material pattern can be sustained.

To understand whether streaming motions are significantly contributing to the TW analysis, we have repeated the procedure using axisymmetric velocity fields built from the output of ROTCUR. We generally find little difference relative to the result for the original velocity field (shown here for the case of NGC 5457 in a plot of  $\langle v \rangle / \langle x \rangle$  vs. aperture number in Figure 2). While this may indicate a limitation of the method, it may alternatively indicate that spiral patterns are in fact close to material patterns. With M. Merrifield, we are pursuing the latter possibility, while with P. Rautiainen we are studying applications of the TW method on simulated spirals with varying pattern speeds and spiral strengths in order to assess the reliability of the method on spiral patterns.

## **References**

- Boselli, A., Lequeux, J., & Gavazzi, G. 2002, *A&A*, 384, 33  
Debattista, V. P. 2003, *MNRAS*, 342, 1194  
Merrifield, M. R., & Kuijken, K. 1995, *MNRAS*, 274, 933  
Pilyugin, L. S., Vilchez, J. M., & Contini, T. 2004, *A&A*, 425, 849  
Rand, R. J. & Wallin, J. F. 2004, *ApJ*, 614, 142  
Roberts, W. & Stewart, G. 1987, *ApJ*, 314, 10  
Tremaine, S. & Weinberg, M. D. 1984, *ApJ*, 282, L5  
Wong, T. & Blitz, L. 2002, *ApJ*, 569, 157  
Zimmer, P., Rand, R. J. & McGraw, J. T. 2004, *ApJ*, 607, 285